

Quantitative Evaluation of Mechanosensing of Cells on Dynamically Tunable Hydrogels

Hiroshi Y. Yoshikawa,^{†,‡} Fernanda F. Rossetti,[†] Stefan Kaufmann,[†] Thomas Kaindl,[†] Jeppe Madsen,[‡] Ulrike Engel,[§] Andrew L. Lewis,^{||} Steven P. Armes,[‡] and Motomu Tanaka^{*,†,⊥}

[†]Physical Chemistry of Biosystems, Institute of Physical Chemistry, University of Heidelberg, D69120 Heidelberg, Germany

[‡]Department of Chemistry, Dainton Building, University of Sheffield, Brook Hill, Sheffield, South Yorkshire, S3 7HF, United Kingdom

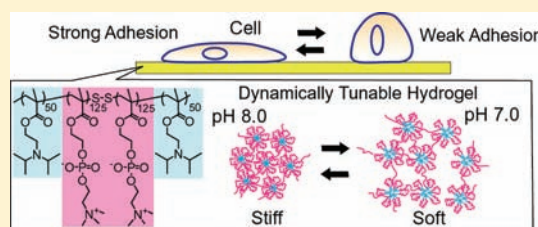
[§]Nikon Imaging Center at the University of Heidelberg, BIOQUANT, D69120 Heidelberg, Germany

^{||}Biocompatibles UK Ltd, Chapman House, Farnham Business Park, Weydon Lane, Farnham, Surrey GU9 8 QL, United Kingdom

[⊥]Cell Biophysics Group, Institute for Toxicology and Genetics, Karlsruhe Institute of Technology, D76131 Karlsruhe, Germany

S Supporting Information

ABSTRACT: Thin hydrogel films based on an ABA triblock copolymer gelator [where A is pH-sensitive poly(2-(diisopropylamino)ethyl methacrylate) (PDPA) and B is biocompatible poly(2-(methacryloyloxy)-ethyl phosphorylcholine) (PMPC)] were used as a stimulus-responsive substrate that allows fine adjustment of the mechanical environment experienced by mouse myoblast cells. The hydrogel film elasticity could be reversibly modulated by a factor of 40 via careful pH adjustment without adversely affecting cell viability. Myoblast cells exhibited pronounced stress fiber formation and flattening on increasing the hydrogel elasticity. As a new tool to evaluate the strength of cell adhesion, we combined a picosecond laser with an inverted microscope and utilized the strong shock wave created by the laser pulse to determine the critical pressure required for cell detachment. Furthermore, we demonstrate that an abrupt jump in the hydrogel elasticity can be utilized to monitor how cells adapt their morphology to changes in their mechanical environment.



INTRODUCTION

In recent years, an increasing number of studies have provided compelling evidence that biological cells have the capability of sensitively responding not only to their biochemical environment but also to their mechanical environment (so-called mechanosensing).^{1,2} Using chemically cross-linked hydrogels as a model for the extracellular matrix (ECM), it has been demonstrated that the elastic properties of substrates play crucial roles in various cellular processes¹ such as morphology^{3–5} and motility^{6,7} of contractile cells and differentiation of mesenchymal stem cells (MSCs).^{8,9} By adjusting the concentration of bifunctional cross-linkers and the reaction time, one can obtain substrates with tunable elastic properties (Young's modulus), which allows the “ex situ” regulation of the mechanical environment experienced by the cells. Recent experiments in vivo or in organ cultures suggest that dynamic changes in the matrix stiffness significantly influence cell behavior during development and disease: the degeneration of γ -irradiated alginate scaffolds enhances the extent of bone regeneration by transplanted stem cells,¹⁰ the stiffening of liver cells due to fibrosis results in significant changes within whole organs,¹¹ and cells switch from a protease-dependent movement to an amoeboid movement in response to the matrix density during tumor metastasis.¹² Complex interplay between these mechanisms required well-defined model systems to better understand how cells respond to matrix stiffness. Hydrogels based on thiolated ECMs

such as hyaluronic acid^{13,14} and gelatin¹⁵ exhibit an increase in elasticity due to disulfide bond formation, and the resulting disulfide cross-links can be degraded by dithiothreitol. However, such a strategy does not allow either reversible cross-linking or degradation cycles. Thus, hydrogels with dynamically tunable mechanical properties open up possibilities for the quantitative investigation of cell responses toward both static and time-dependent mechanical stresses.

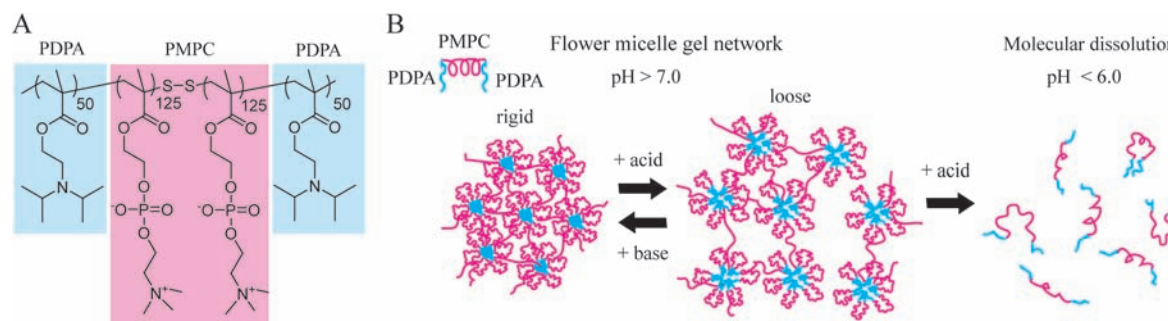
Previously, we deposited a diblock copolymer monolayer based on poly(2-(dimethylamino)ethyl methacrylate-*block*-methyl methacrylate) (PDMAEMA-PMMA), which comprises an equal number of monomer repeat units ($n = 36$) for the hydrophobic PMMA and pH-responsive PDMAEMA blocks, from the air/water interface onto a hydrophobic solid substrate.^{16,17} Specular neutron reflectivity experiments in the presence and in the absence of a biological membrane model (supported lipid membrane) demonstrated that the PDMAEMA brushes reversibly change their conformation by pH modulation,¹⁶ which results in a significant variation in the membrane–substrate interaction.¹⁷

In this study, we utilized a copolymer hydrogel that exhibits a substantial change in its viscoelastic response with subtle changes

Received: July 8, 2010

Published: January 10, 2011

Scheme 1. (A) Chemical Structure of the pH-Sensitive PDPA₅₀-PMPC₂₅₀-PDPA₅₀ Triblock Copolymer Used in This Work and (B) Schematic Representation of the Structural Changes That Occur within the Micellar Gel Network on Adjusting the Gel pH by the Addition of Either Acid or Base



in solution pH.^{18,19} From various triblock copolymers that are known to be responsive to external stimuli (temperature, pH, etc.),^{18–23} we selected a highly biocompatible pH-responsive ABA-type triblock copolymer [where A is poly-(2-(diisopropylamino)ethyl methacrylate)] (PDPA) and B is poly(2-(methacryloyloxy)ethyl phosphorylcholine) (PMPC)] (Scheme 1A) in order to minimize any reduction in cell viability. Since PDPA is a weak polyelectrolyte (the pK_a of protonated PDPA homopolymer is around pH 6.2),²⁴ the mean degree of ionization of the outer PDPA blocks (mean degree of polymerization, $n = 50$) decreases as the pH is increased.¹⁸ The central MPC block (for which $n = 250$) confers excellent biocompatibility.^{21,23,25,26} As schematically shown in Scheme 1B, PDPA₅₀-PMPC₂₅₀-PDPA₅₀ triblock copolymer forms a free-standing transparent gel comprising a 3D network of interconnected “flower” micelles above pH 7. At higher gel pH, the PDPA chains become more deprotonated and hence more hydrophobic. This leads to stronger interchain interactions, resulting in a highly elastic, physically cross-linked hydrogel film. On lowering the gel pH, the hydrophobic interaction between the now partially charged PDPA blocks (and thus the physical cross-linking) becomes much weaker, which results in a softer gel film. Finally, the triblock copolymer chains become molecularly dissolved below pH 6.

In this study, we prepared dry copolymer films by spin-coating methanolic PDPA₅₀-PMPC₂₅₀-PDPA₅₀ solutions. On immersion in water, the thickness of the resulting swollen hydrogel films was 3–4 μm (see the Supporting Information, Figure S1). In contrast to our previous work on diblock copolymer monolayers of less than 10 nm,^{16,17} these relatively thick films allow us to significantly reduce the influence of the underlying substrate on the cell behavior. On the basis of the range of the film elasticity determined by the nanoindentation method,^{27,28} we selected mouse myoblast (C2C12) cells for evaluation, since their contact tissues possess comparable elasticity to the copolymer gel films.⁴

In addition to the analysis of cell shape using bright-field and confocal microscopy, we developed a new technique to measure the strength of cell adhesion using pressure waves induced by intensive picosecond laser pulses. The pressure that can be exerted on a cell ($\sim\text{MPa}$) is strong enough to cause cell detachment, which is approximately 6 orders of magnitude larger than the typical force range achieved with optical traps²⁹ and magnetic tweezers.³⁰ As the applied pressure can be calibrated from knowledge of the laser energy and the distance between the focal point and the target, the critical pressure required for cell

detachment can be determined quantitatively. In contrast to alternative approaches such as pulling a magnetic particle attached to a cell³⁰ or peeling off a cell from its contacting substrate using an AFM tip,³¹ our strategy is a probe-free technique that enables reliable statistics from many cells to be obtained.

EXPERIMENTAL SECTION

Experimental details for all materials used, the synthesis of PDPA₅₀-PMPC₂₅₀-PDPA₅₀ triblock copolymer, preparation of PDPA₅₀-PMPC₂₅₀-PDPA₅₀ triblock copolymer hydrogel films, evaluation of adsorption of bovine serum albumin (BSA) onto triblock copolymer hydrogels, nanoindentation of triblock copolymer hydrogels, cell culture, area and shape analysis of cells, confocal microscopy of immunofluorescence, and cell viability and proliferation assays are provided in the Supporting Information.

Picosecond Laser Detachment Assay. A picosecond Nd:YAG laser system ($\lambda = 1064 \text{ nm}$, $\tau_L = 60 \text{ ps}$, PY 61C-20, Continuum, Santa Clara, CA) was used to induce shock waves. The picosecond laser pulses were led through the inverted microscope and focused through a 20 \times objective lens (N.A. = 0.75, Nikon Instruments Inc.). A single picosecond laser pulse was focused into the culture medium at a fixed distance of 2 mm from cells and 100 μm above the hydrogel surface. The laser energy was adjusted with a polarizer and measured with a power meter (PE 10-S, OPHIR). The minimum energy needed to detach cells from substrate is the critical detachment energy. This parameter was determined empirically by systematically varying the detachment energy until the minimum threshold value was achieved for cell detachment from the substrate. The corresponding critical pressure (i.e., the minimum pressure required for cell detachment) was then calculated from the energy–pressure curve obtained in water using a factory-calibrated pressure sensor (Müller-Platte Needleprobe, Müller Instruments, Oberursel, Germany) (see the Supporting Information, Figures S2 and S3).

RESULTS AND DISCUSSION

Elastic Properties of PDPA₅₀-PMPC₂₅₀-PDPA₅₀ Triblock Copolymer Hydrogel Films. Young's moduli, E , of the PDPA₅₀-PMPC₂₅₀-PDPA₅₀ triblock copolymer hydrogel films were calculated from the force–indentation curves using the modified Hertz model.^{32,33} The Hertz model can be applied to thin films, provided that the indentation into the sample by the tip is sufficiently small compared to the film thickness. Thus, the fitting analysis was confined to the first 5–100 nm (i.e., less than 10% of the thickness of the hydrated films) of the f – i curves to determine E values that were independent of the underlying stiff glass substrate.^{27,28} In fact,

the $f-i$ curves provide a good fit to the Hertz model over a somewhat wider range ($i = 0-200$ nm). Figure 1 shows the Young's modulus measured at different solution pH values. The Young's modulus of the hydrogels can be reversibly tuned from 1.4 to 40 kPa simply by adjusting the pH from 7.0 to 8.0. This range covers the optimal elasticity not only for muscle cells (~ 10 kPa) but also for neurons (~ 1 kPa), suggesting that these hydrogel films have the potential to enable various cell types to be cultured.^{8,9,34}

Changes in Cell Morphology and Shapes. Figure 2A–C, E–G shows the characteristic morphology of mouse myoblast (C2C12) cells cultured on the hydrogels with different elastic moduli, $E = 1.4$ (pH 7.0), 19 (pH 7.5), and 40 kPa (pH 8.0), for 3 and 24 h. For comparison, the shapes of these cells when placed on a bare glass substrate ($E \approx 50$ GPa) are presented in Figure 3D,H. The staining of actin with Alexa 488-conjugated

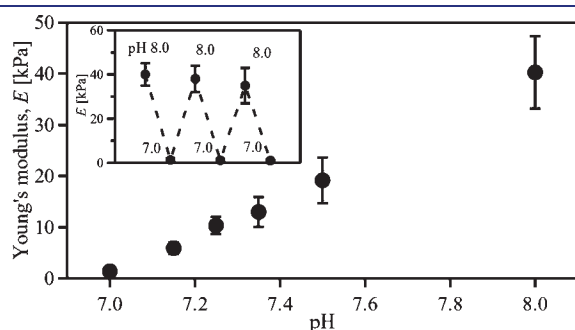


Figure 1. Young's modulus, E , determined for triblock copolymer hydrogel films at various gel pH values. The Young's modulus was calculated from the force–indentation curves using a modified Hertz model. The inset illustrates the reversible modulation of E values over several pH cycles.

phalloidin reveals that more pronounced stress fiber formation and flattening of the cells occurs on copolymer gel films with a relatively high elastic modulus (pH 8.0), while C2C12 cells adopt a hemispherical shape on a softer copolymer gel film (pH 7.0). It should be noted that the different cell shapes observed here are not attributed to any change in cell viability because no significant differences in either the cell shape or viability were observed for experiments conducted on either plastic or glass substrates from pH 7.0 to 8.0 (see the Supporting Information, Figures S4–S6). Furthermore, our picosecond laser detachment assay confirmed that the strength of cell adhesion on glass substrates was not altered by adjusting the pH (see below for further details). Possible electrostatic interaction effects can also be discounted, because the PDPA block is slightly more cationic at pH 7.0, and thus should be more strongly electrostatically attracted to cells covered with negatively charged glycocalyx. In fact, the cells exhibited the most pronounced spreading over a bare anionic glass substrate, which is electrostatically repulsive to cell glycocalyx. The influence of serum protein adsorption on cell adhesion can be negligible, because cells displayed no difference in spreading between the hydrogels, whose overnight immersion prior to cell culture was conducted either in HEPES buffer solution (no serum) or in culture media (with serum) (see the Supporting Information, Figure S7). In addition, we found no difference in bovine serum albumin (BSA) adsorption onto the hydrogel films over the whole pH range used in this study (see the Supporting Information, Figure S8). Actually, it was reported that surface coatings based on MPC-based copolymers lead to a significant reduction in the adsorption of blood proteins such as albumin and fibrinogen.^{26,35} Thus, it is evident that the hydrogel elasticity has a major impact on the cell morphology.

Recent studies of MSCs on soft hydrogels ($E \approx 1$ kPa) indicate that MSCs can “feel” the underlying substrate up to a depth of

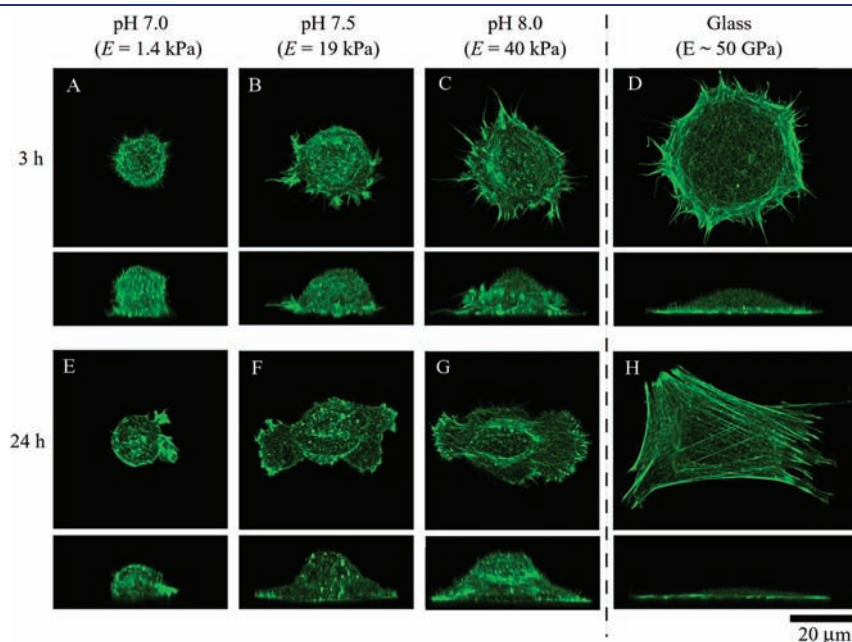


Figure 2. Confocal fluorescence images obtained for C2C12 cells on triblock copolymer films after 3 (upper rows) and 24 h (lower rows) at $E = 1.4$ (pH 7.0), 19 (pH 7.5), and 40 kPa (pH 8.0). Prior to imaging, the cells were fixed and stained with Alexa 488 phalloidin. More pronounced flattening of cells and remodeling of cytoskeletons were observed for higher hydrogel elasticities. For reference purposes, the corresponding images obtained for a bare glass substrate ($E \approx 50$ GPa) are presented in the right-hand column. The images represent maximal projection along the optical axis (z -axis, top) and a side projection (y -axis, side).

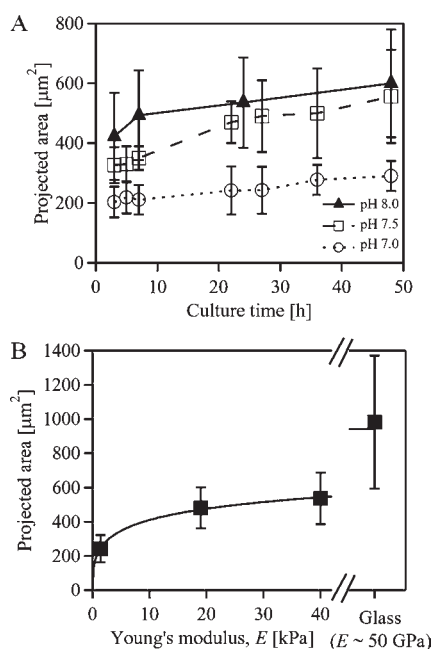


Figure 3. Projected area of C2C12 cells on triblock copolymer hydrogels as a function of (A) time and (B) the elastic modulus of the substrate ($t \approx 24$ h). The total number of cells for each data point is 50. Error bars represent the standard deviations.

$3.4 \mu\text{m}$.^{36,37} Notwithstanding the different cell types, this suggests that the C2C12 cells on our hydrogels may be decoupled from the glass substrate. In fact, we found that C2C12 cells adopt a round shape on a soft copolymer gel film ($E \approx 1$ kPa), which is comparable to data reported in a previous study.⁴ Thus, we feel justified in concluding that the C2C12 cells are most likely not significantly influenced by the underlying substrate in the present study.

From bright-field images, we further evaluated the dependence of the projected area on the hydrogel elasticity as a function of time (Figure 3A). After incubation for 3 h, significant differences in spreading behavior were already discernible: the projected area of cells ($423 \pm 160 \mu\text{m}^2$) on a stiff hydrogel ($E = 40$ kPa) is about twice that observed ($203 \pm 49 \mu\text{m}^2$) on a soft hydrogel ($E = 1.4$ kPa). It is also noteworthy that the projected area of cells in contact with the bare glass substrate ($750 \pm 393 \mu\text{m}^2$) is only around a factor of 2 larger than that on the stiff hydrogel, although the elastic modulus for glass ($E \approx 50$ GPa) is approximately 6 orders of magnitude larger. To obtain more quantitative insights regarding the asymptotic behavior of cell spreading, a hyperbolic fit of projected cell area versus substrate stiffness near the saturation level ($t \approx 24$ h) is presented in Figure 3B. The solid line in the figure is the fit according to the empirical Hill equation:^{3,4}

$$\text{area} = aE^m / [(E_{1/2\text{-spread}})^m + E^m] \quad (1)$$

where $E_{1/2\text{-spread}}$ is the half-saturation constant for cell spreading and m is the cooperativity coefficient in the Hill equation. In our system, we obtained $E_{1/2\text{-spread}} = 23$ kPa and $m = 0.39$. $E_{1/2\text{-spread}}$ can be used as a criterion for cell spreading: substrates with $E \geq E_{1/2\text{-spread}}$ facilitate cell spreading, while softer substrates ($E < E_{1/2\text{-spread}}$) elicit little cell spreading. A cooperativity coefficient smaller than unity ($m = 0.39$) indicates that the cooperativity is negative, which can be attributed to the fact that PDPA₅₀-PMPC₂₅₀-PDPA₅₀ triblock copolymer contains no specific biochemical

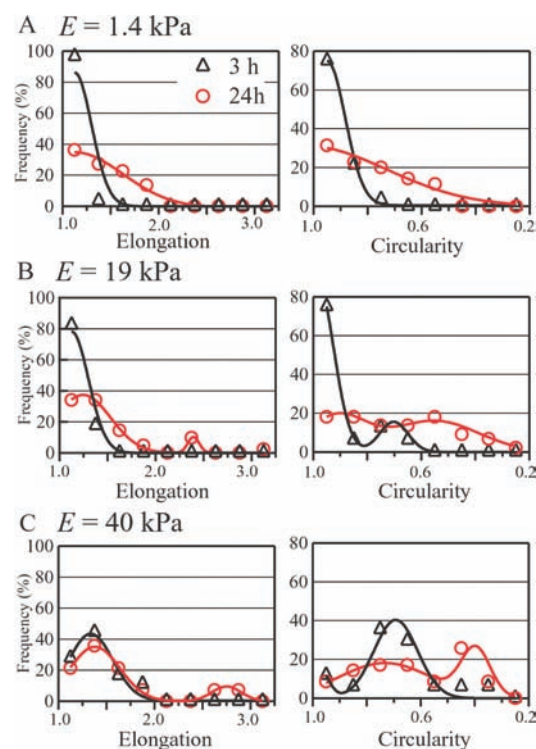


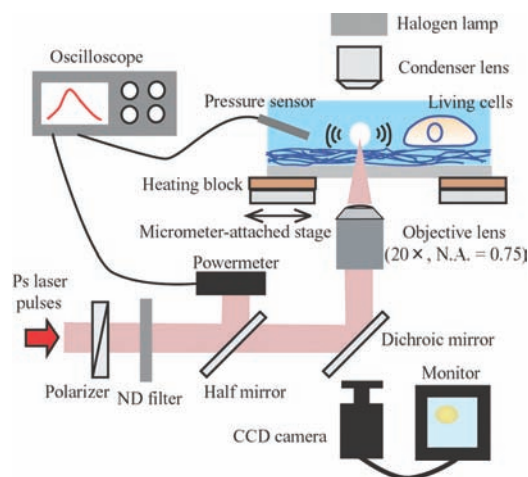
Figure 4. Histograms of elongation (the ratio between minor and major axes) and circularity ($\text{perimeter}^2 / (4\pi^2 \times \text{projected area})$) of cells on triblock copolymer hydrogel films at $E =$ (A) 1.4 (pH 7.0), (B) 19 (pH 7.5), and (C) 40 kPa (pH 8.0), recorded after 3 (black) and 24 h (red) of incubation. The solid lines represent fits to the histograms using either single or double Gaussian functions. An increase in the substrate elasticity leads to the elongation and flattening of cells, which becomes more prominent with time.

ligand. Previously, Discher et al. reported $E_{1/2\text{-spread}} = 2.5$ kPa and $m \approx 1$ for C2C12 cells on polyacrylamide (PA) gels functionalized with collagen.⁴ The difference between our experimental findings and the results of Discher et al. can be attributed to the fact that our triblocks have no specific binding motifs in the side chains (such as collagen). In fact, comparing the area of C2C12 cells on two hydrogels with comparable elasticity ($E \approx 1$ kPa), we found the cell contact area is approximately 2–3 times larger on the collagen-coated PA gels.⁴

In addition to our analysis of the cell contact area, we evaluated two other important structural parameters, cell elongation and circularity. The former is simply the length/width ratio of a cell defined within a minimum bounding box, while the latter is defined as $4\pi(\text{projected area}) / (\text{perimeter})^2$. Figure 4 represents the histograms of elongation and circularity calculated from an analysis of more than 50 C2C12 cells on hydrogels with $E =$ (A) 1.4, (B) 19, and (C) 40 kPa. The histogram of these structural parameters for the softer hydrogel surface (A) is rather well-fitted using a single Gaussian function, whereas the histograms obtained for the two stiffer surfaces (B,C) are well-fitted with double Gaussian functions. The secondary populations, which correspond to pronounced elongation and low circularity, become more prominent on increasing the substrate elasticity. This is in contrast to cells deposited on the softer surface, where spreading is less pronounced and more isotropic.

Quantitative Measurements of Cell Adhesion Strength. To evaluate the strength of cell adhesion on these synthetic

Scheme 2. Schematic Illustration of a Picosecond Laser Coupled to an Inverted Microscope Equipped with a Cell Incubation Chamber^a



^a Pressures generated by laser pulses can be calibrated by the pulse energy and the distance between the focal point and the target cell, which enables the cell adhesion strength to be determined.

triblock copolymer hydrogels, we utilized pressure waves induced by picosecond laser pulses. As shown in Scheme 2, the pressure wave induced by a picosecond laser pulse is exerted on a cell. The magnitude of such pressure waves was monitored using a pressure sensor (see Figure S2). The first pressure wave (full width at a half-maximum ≈ 80 ns) had a supersonic velocity of approximately 1640 m s^{-1} . Since this “shock wave” proved to be the strongest within the whole time window, it is the dominant cell detachment force in the following experiments. As presented in Figure S3, the pressure generated by a shock wave can be calibrated by the laser pulse energy and the distance from the focus. The critical pressures required to cause the detachment of adherent cells can be readily calculated by careful calibration prior to the experiments. C2C12 cells adhered on either soft or elastic hydrogels could be detached using laser-induced shock waves that correspond to pressures of either 1.1 or 2.0 MPa, respectively (Figure 5). It should be emphasized that the detachment caused by the shock wave did not result in cell death (e.g., ejection of cytoplasm). Moreover, there were no signs of any debris remaining on the hydrogel surfaces after cell detachment. Indeed, the detached cells could adhere and continue to grow once contact with the hydrogel surface was re-established.

The irradiation of an intensive, short laser pulse often leads to the generation of a cavitation bubble, which is known to cause tissue damage in laser medical surgeries.³⁸ In our study, we carefully excluded any potential damage to the target cells by cavitation bubbles. First, the distance between the cells and the laser focal point (2.0 mm) was set larger than the maximum radius of cavitation bubbles ($R_{\text{max}} < 1.4$ mm) and the film damage ($R_{\text{damage}} < 300 \mu\text{m}$) achievable using our setup (see the Supporting Information, Figure S9). Second, the short separation distance between the cavity inception and the substrate (~ 0.1 mm) suppresses any adverse effects due to hydrodynamic liquid jet impacts.^{39,40} Thus, the target cells are not exposed to hot gaseous products from the medium-to-strong hydrodynamic liquid jets.

Figure 6 shows time courses for the critical shock wave pressures required for cell detachment from the hydrogel surface.

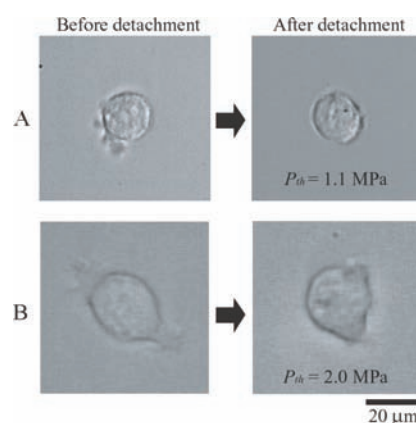


Figure 5. (A) Bright-field images of an individual cell on a soft hydrogel ($E = 1.4$ kPa, pH 7) before (left) and after (right) its detachment when subjected to a shock wave above a certain minimum pressure. Note that the detached cell is shifted by about $10 \mu\text{m}$ due to its inertia until it adheres to the film again. (B) The corresponding result obtained for a stiff gel ($E = 40$ kPa, pH 8) also confirms that cells that are exposed to a high-pressure shock wave (>1 MPa) remain active, retaining their capability to adhere once more to the hydrogel surface and even continue their growth at this new location.

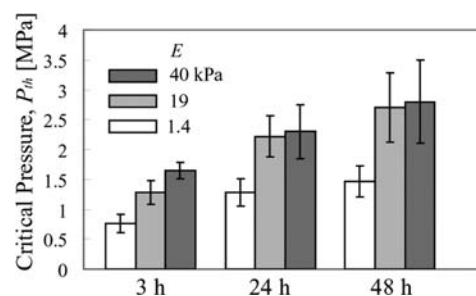


Figure 6. Time courses for a critical shock wave pressure, P_{th} , required to cause cell detachment from triblock copolymer hydrogel films. The error bar represents standard deviation. The total number of cells for each data point is 50.

The results obtained after 3 h clearly indicate that the critical pressure increases monotonically with the elastic modulus: $P_{\text{th}} = 0.77, 1.3,$ and 1.6 MPa for $E = 1.4, 19,$ and 40 kPa, respectively. We also observed that the P_{th} values increase continuously with time, regardless of the film elasticity. This trend can be directly correlated with the cell adhesion behavior presented in Figures 2–4. For higher hydrogel elasticities, C2C12 cells show more pronounced spreading and stress fiber formation. Actually, the critical pressures ($P_{\text{th}} \approx 10$ MPa) determined for cell detachment from glass substrates ($E \approx 50$ GPa, pH 7–8) are about 7 times larger than the corresponding values determined for hydrogels. After 24 h, the P_{th} value of 2.2 MPa obtained at pH 7.5 ($E = 19$ kPa) is very close to that observed at pH 8.0 ($E = 40$ kPa), which seems to be consistent with the comparable projected areas for these two conditions (Figure 3A). Interestingly, both the projected area and the P_{th} of cells at pH 7.0 ($E = 1.4$ kPa) are almost 50% of the corresponding values obtained at pH 7.5 and 8.0.

Previously, Hosokawa et al. proposed that shock waves induced by femtosecond laser pulses can be used for manipulation (detachment and sorting) of fibroblasts on cell culture dishes with/without fibronectin coating, once filopodia are cut

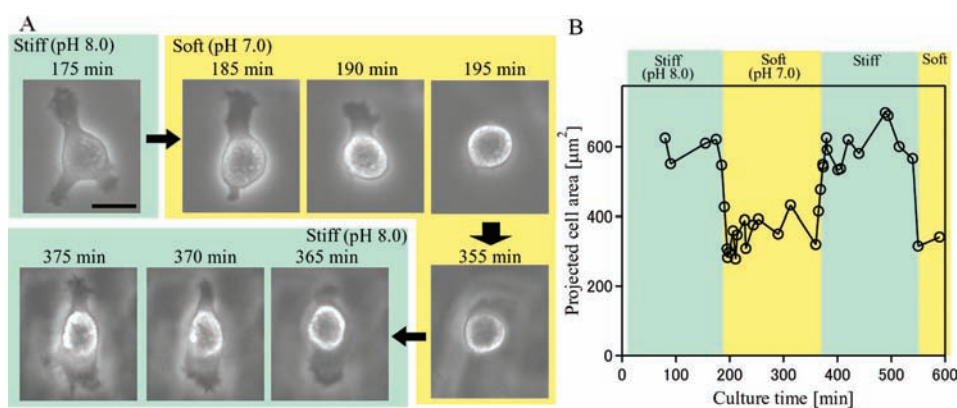


Figure 7. Dynamic response of a cell to elasticity changes caused by exchanging culture media at 180 (pH 8.0 → 7.0), 360 (pH 7.0 → 8.0), and 540 min (pH 8.0 → 7.0). (A) Phase contrast images obtained for cells during these changes in dynamic hydrogel elasticity (scale bar: 20 μm). (B) Time evolution of the projected area of the observed cell calculated from the images presented in (A).

prior to the shock wave experiments.⁴¹ Hagerman and co-workers proposed applying pressure waves perpendicular to the surfaces by illuminating the substrate from the back side.^{42,43} Despite using different target cells as well as varying physical and biochemical properties of substrates, the reported values seem to be of the same order of magnitude as those in the present study. On the other hand, if one roughly assumes that the area of a C2C12 cell exposed to a shock wave is about 100 μm², one can estimate the critical detachment force f_{th} to be ~100 μN. This is more than 2–3 orders of magnitude larger than the lateral “peel-off” force for C2C12 cells measured using micropipets, $f_{th} \approx 0.05 \mu\text{N}$,⁴⁴ and for fibroblasts measured using AFM, $f_{th} \approx 0.4 \mu\text{N}$.³¹ However, one major difference between the shock waves method and other experiments (micropipets and AFM) is the duration of the mechanical stimulus (note that the duration of the shock waves used in this study is about 80 ns), resulting in a significant difference in loading rates. As demonstrated by the AFM experiments reported by Merkel et al.,⁴⁵ higher loading rates result in stronger interactions between ligand–receptor pairs. If one converts the loading rates (10⁶ s^{−1}) into a stress (which is of the order of MPa),^{42,43} this has the same order of magnitude as the critical pressure determined in the present study. Furthermore, cell deformation by shock waves should be predominantly elastic within such a short time frame,⁴⁶ which could result in a different detachment mechanism compared to the continuous “peeling” of cells using an AFM cantilever.

Mechanosensing of Cells upon Dynamic Change in Mechanical Environment. One unique advantage offered by these pH-sensitive PDPA₅₀-PMPC₂₅₀-PDPA₅₀ hydrogels is the ability to dynamically tune their mechanical properties simply by adjusting the solution pH. To observe the dynamic response of cells to their mechanical environment, we varied the solution pH of the culture medium between 8.0 and 7.0 every 180 min. Figure 7A shows the representative phase contrast images obtained for a single C2C12 cell responding to several pH cycles. During the first 180 min period at pH 8.0, the C2C12 cell became stretched and flattened on a stiff surface ($E = 40$ kPa). Upon adjusting the pH to 7.0 at $t = 180$ min, the cell began to shrink and became round within 15 min, which is comparable to observations made for relatively soft hydrogels ($E \approx 1$ kPa). Interestingly, adjusting the pH to 8.0 at $t = 360$ min (thus stiffening the hydrogel) led to an immediate transition to produce a stretched cell within 15 min. The observed changes in cell morphology were evaluated by monitoring the projected area of the cell as a

function of time (Figure 7B), showing sharp and reversible transitions between the round state (projected area ~300 μm²) and the stretched state (~600 μm²) corresponding to the soft ($E = 1.4$ kPa) and elastic ($E = 40$ kPa) nature of the hydrogels.

Although the local pH in the hydrogel films could not be monitored directly, proton diffusion in or out of the hydrogel ($D > 10^2 \mu\text{m}^2/\text{s}$) should enable the equilibrium hydrogel elasticity to be achieved much faster than the typical time scale of ~10 min that is required to observe changes in the cell shape. Thus, the time trace of the projected area can be regarded as the relaxation of adhering cells responding to an abrupt jump in the hydrogel elasticity. Since there are no specific interactions between the cells and the hydrogel surface, it is plausible that the observed shape transition is governed by the remodeling of the cytoskeleton but not by the association/dissociation of ligand–receptor pairs. Our experimental results provide clear evidence that the change in the mechanical environment quickly triggers changes in the cell morphology with no significant time lag. The characteristic time for the increase in the contact area observed for stiffer hydrogels seems to be comparable to that found in the early stages of cell adhesion.^{47–49} Cuvelier et al. reported that the contact radius, R , of HeLa cells follows a fast initial diffusive regime according to the scaling law $R \sim t^{1/2}$, and subsequently slows to a subdiffusive behavior summarized by the scaling law $R \sim t^{1/4}$.⁴⁷ The sharp transition between two distinct cell states (i.e., their stretched and round shapes) suggests that cells undergo a first-order phase transition between strong and weak adhesion.^{50–52} Recently, Besser and Schwarz have predicted the hysteresis in the mechanosensing of cells to dynamic changes in the substrate elasticity.⁵³ Thus, the novel use of the stimulus-responsive polymer hydrogel described in the present study allows us to gain deeper insights into the cell morphology responding to dynamic (and thus time-dependent) mechanical cues.

CONCLUSIONS

Thin hydrogel films based on an ABA triblock copolymer containing biocompatible 2-(methacryloyloxy)ethyl phosphorylcholine (MPC) and pH-sensitive 2-(diisopropylamino)ethyl methacrylate] (DPA) blocks are shown to be a versatile new synthetic platform that enables cell behavior to be fine-tuned. Indentation experiments confirm that the elasticity of such hydrogels could be conveniently tuned over a wide range

(Young's modulus = 1.4–40 kPa) simply by adjusting the solution pH over a relatively narrow, physiologically relevant range (pH 7–8). Confocal microscopy images of mouse myoblast cells indicate clear differences in cell morphology: pronounced stress fiber formation and flattening of the cells was observed for a hydrogel film with a relatively high elastic modulus ($E \approx 40$ kPa). Using strong shock waves generated by picosecond laser pulses, the strength of cell adhesion could be quantitatively assessed by determining the critical pressures required for cell detachment. Moreover, it has been demonstrated that this synthetic stimulus-responsive hydrogel allows the dynamic modulation of cell–substrate contacts, which enables one to monitor the morphological transition of cells caused by time-dependent mechanical stresses. These results indicate the potential of stimulus-responsive hydrogel films for the detailed investigation of both ex situ and in situ mechanosensing of contractile cells responding to external stimuli in their surrounding environment. Judicious use of a synthetic pH-responsive triblock copolymer gelator has enabled us to obtain new insights into the mechanism of mechanosensing of contractile cells. This is a good example of how cutting-edge synthetic chemistry can facilitate important new physical insights in biophysics and cell biology.

■ ASSOCIATED CONTENT

S Supporting Information. Experimental Section, influence of solution pH on cell viability, and estimation of the maximum radius of a cavitation bubble. This material is available free of charge via the Internet at <http://pubs.acs.org>.

■ AUTHOR INFORMATION

Corresponding Author
tanaka@uni-heidelberg.de

Present Addresses

*Physics Department, St. Francis Xavier University, Antigonish, Nova Scotia, Canada B2G 2W5

■ ACKNOWLEDGMENT

We thank Dr. C. Ackermann for experimental assistance at the Nikon Imaging Center at the University of Heidelberg and Prof. U. Schwarz for stimulating discussions. M.T. and U.E. are the members of the German Excellence Cluster “Cell Network” and BIOQUANT. M.T. is thankful to the Helmholtz Society for support through the “BioInterface” program. H.Y.Y. thanks the Alexander von Humboldt Foundation for a research fellowship. S.P.A. is the recipient of a Royal Society-Wolfson Research Merit award, and J.M. thanks EPSRC for postdoctoral support. Bio-compatibles UK Ltd. is thanked for the kind donation of the MPC monomer and for permission to publish this work.

■ REFERENCES

- (1) Discher, D. E.; Janmey, P.; Wang, Y. L. *Science* **2005**, *310*, 1139.
- (2) Vogel, V.; Sheetz, M. *Nat. Rev. Mol. Cell Biol.* **2006**, *7*, 265.
- (3) Engler, A.; Bacakova, L.; Newman, C.; Hategan, A.; Griffin, M.; Discher, D. *Biophys. J.* **2004**, *86*, 388a.
- (4) Engler, A. J.; Griffin, M. A.; Sen, S.; Bonnetmann, C. G.; Sweeney, H. L.; Discher, D. E. *J. Cell Biol.* **2004**, *166*, 877.
- (5) Georges, P. C.; Miller, W. J.; Meaney, D. F.; Sawyer, E. S.; Janmey, P. A. *Biophys. J.* **2006**, *90*, 3012.
- (6) Lo, C. M.; Wang, H. B.; Dembo, M.; Wang, Y. L. *Biophys. J.* **2000**, *79*, 144.
- (7) Gray, D. S.; Tien, J.; Chen, C. S. *J. Biomed. Mater. Res. A* **2003**, *66A*, 605.
- (8) Engler, A. J.; Sen, S.; Sweeney, H. L.; Discher, D. E. *Cell* **2006**, *126*, 677.
- (9) Discher, D. E.; Mooney, D. J.; Zandstra, P. W. *Science* **2009**, *324*, 1673.
- (10) Simmons, C. A.; Alsberg, E.; Hsiong, S.; Kim, W. J.; Mooney, D. J. *Bone* **2004**, *35*, 562.
- (11) Wells, R. G. *Hepatology* **2008**, *47*, 1394.
- (12) Wolf, K.; Mazo, I.; Leung, H.; Engelke, K.; von Andrian, U. H.; Deryugina, E. I.; Strongin, A. Y.; Brocker, E. B.; Friedl, P. *J. Cell Biol.* **2003**, *160*, 267.
- (13) Shu, X. Z.; Liu, Y. C.; Luo, Y.; Roberts, M. C.; Prestwich, G. D. *Biomacromolecules* **2002**, *3*, 1304.
- (14) Engler, A. J.; Rehfeldt, F.; Sen, S.; Discher, D. E. *Methods Cell Biol.* **2007**, *83*, 521.
- (15) Shu, X. Z.; Ahmad, S.; Liu, Y. C.; Prestwich, G. D. *J. Biomed. Mater. Res. A* **2006**, *79A*, 902.
- (16) Rehfeldt, F.; Steitz, R.; Armes, S. P.; Von Klitzing, R.; Gast, A. P.; Tanaka, M. *J. Phys. Chem. B* **2006**, *110*, 9171.
- (17) Rehfeldt, F.; Steitz, R.; Armes, S. P.; von Klitzing, R.; Gast, A. P.; Tanaka, M. *J. Phys. Chem. B* **2006**, *110*, 9177.
- (18) Ma, Y. H.; Tang, Y. Q.; Billingham, N. C.; Armes, S. P.; Lewis, A. L. *Biomacromolecules* **2003**, *4*, 864.
- (19) Castelletto, V.; Hamley, I. W.; Ma, Y. H.; Bories-Azeau, X.; Armes, S. P.; Lewis, A. L. *Langmuir* **2004**, *20*, 4306.
- (20) Madsen, J.; Armes, S. P.; Lewis, A. L. *Macromolecules* **2006**, *39*, 7455.
- (21) Li, C. M.; Tang, Y. Q.; Armes, S. P.; Morris, C. J.; Rose, S. F.; Lloyd, A. W.; Lewis, A. L. *Biomacromolecules* **2005**, *6*, 994.
- (22) Li, C. M.; Madsen, J.; Armes, S. P.; Lewis, A. L. *Angew. Chem., Int. Ed.* **2006**, *45*, 3510.
- (23) Madsen, J.; Armes, S. P.; Bertal, K.; Lomas, H.; MacNeil, S.; Lewis, A. L. *Biomacromolecules* **2008**, *9*, 2265.
- (24) Butun, V.; Armes, S. P.; Billingham, N. C. *Polymer* **2001**, *42*, 5993.
- (25) Lewis, A. L. *Colloids Surf. B* **2000**, *18*, 261.
- (26) Iwasaki, Y.; Ishihara, K. *Anal. Bioanal. Chem.* **2005**, *381*, 534.
- (27) Domke, J.; Radmacher, M. *Langmuir* **1998**, *14*, 3320.
- (28) Rotsch, C.; Jacobson, K.; Radmacher, M. *Proc. Natl. Acad. Sci. U.S.A.* **1999**, *96*, 921.
- (29) Finer, J. T.; Simmons, R. M.; Spudich, J. A. *Nature* **1994**, *368*, 113.
- (30) Bausch, A. R.; Moller, W.; Sackmann, E. *Biophys. J.* **1999**, *76*, 573.
- (31) Yamamoto, A.; Mishima, S.; Maruyama, N.; Sumita, M. *Bio-materials* **1998**, *19*, 871.
- (32) Sneddon, I. N. *Int. J. Eng. Sci.* **1965**, *3*, 47.
- (33) Hertz, H. *J. Reine Angew. Math.* **1882**, *92*, 156.
- (34) Engler, A. J.; Carag-Krieger, C.; Johnson, C. P.; Raab, M.; Tang, H. Y.; Speicher, D. W.; Sanger, J. W.; Sanger, J. M.; Discher, D. E. *J. Cell Sci.* **2008**, *121*, 3794.
- (35) Lu, J. R.; Murphy, E. F.; Su, T. J.; Lewis, A. L.; Stratford, P. W.; Satija, S. K. *Langmuir* **2001**, *17*, 3382.
- (36) Buxboim, A.; Ivanovska, I. L.; Discher, D. E. *J. Cell. Sci.* **2010**, *123*, 297.
- (37) Buxboim, A.; Rajagopal, K.; Brown, A. E. X.; Discher, D. E. *J. Phys.-Condens. Matter* **2010** in press.
- (38) Vogel, A.; Busch, S.; Parltitz, U. *J. Acoust. Soc. Am.* **1996**, *100*, 148.
- (39) Vogel, A.; Lauterborn, W.; Timm, R. *J. Fluid Mech.* **1989**, *206*, 299.
- (40) Zhao, R.; Liang, Z. C.; Xu, R. Q.; Lu, J.; Ni, X. W. *Jpn. J. Appl. Phys.* **2008**, *47*, 5482.
- (41) Hosokawa, Y.; Takabayashi, H.; Miura, S.; Shukunami, C.; Hiraki, Y.; Masuhara, H. *Appl. Phys. A: Mater. Sci. Process.* **2004**, *79*, 795.

- (42) Hagerman, E.; Shim, J.; Gupta, V.; Wu, B. *J. Biomed. Mater. Res. A* **2007**, *82A*, 852.
- (43) Shim, J.; Hagerman, E.; Wu, B.; Gupta, V. *Acta Biomater.* **2008**, *4*, 1657.
- (44) Griffin, M. A.; Engler, A. J.; Barber, T. A.; Healy, K. E.; Sweeney, H. L.; Discher, D. E. *Biophys. J.* **2004**, *86*, 1209.
- (45) Merkel, R.; Nassoy, P.; Leung, A.; Ritchie, K.; Evans, E. *Nature* **1999**, *397*, 50.
- (46) Engelhardt, H.; Sackmann, E. *Biophys. J.* **1988**, *54*, 495.
- (47) Cuvelier, D.; Thery, M.; Chu, Y. S.; Dufour, S.; Thiery, J. P.; Bornens, M.; Nassoy, P.; Mahadevan, L. *Curr. Biol.* **2007**, *17*, 694.
- (48) Dobreiner, H. G.; Dubin-Thaler, B.; Giannone, G.; Xenias, H. S.; Sheetz, M. P. *Phys. Rev. Lett.* **2004**, *93*, 108105.
- (49) Li, Y.; Xu, G. K.; Li, B.; Feng, X. Q. *Appl. Phys. Lett.* **2010**, *96*, No. 043703.
- (50) Bruinsma, R.; Behrisch, A.; Sackmann, E. *Phys. Rev. E* **2000**, *61*, 4253.
- (51) Guttenberg, Z.; Lorz, B.; Sackmann, E.; Boulbitch, A. *Europhys. Lett.* **2001**, *54*, 826.
- (52) Sackmann, E.; Bruinsma, R. F. *ChemPhysChem* **2002**, *3*, 262.
- (53) Besser, A.; Schwarz, U. S. *Biophys. J.* **2010**, *99*, L10.